Hindawi
International Journal of Aerospace Engineering
Volume 2021, Article ID 6665869, 13 pages
https://doi.org/10.1155/2021/6665869

Research Article

Performance Prediction Model of Dynamic Pressure Oil-Air Separator

Xiaobin Zhang,[1] **Lei Lang**,[1] **Xiaofeng Zhang**,[1] **Hongqing Lv**,[1] **and Na Gao**[2]

[1]*College of Aerospace and Civil Engineering, Harbin Engineering University, Harbin 150001, China*
[2]*Avic Aerodynamics Research Institute, Harbin 150001, China*

Correspondence should be addressed to Lei Lang; langlei@hrbeu.edu.cn

Received 27 October 2020; Revised 21 December 2020; Accepted 18 January 2021; Published 10 February 2021

Academic Editor: Rosario Pecora

Based on the aeroengine lubricating oil system test bench, this paper used a dimensional analysis method to establish a mathematical model for predicting the separation efficiency and resistance of a dynamic pressure oil-air separator suitable for engineering. The analysis of the multivariate nonlinear fitting error and the experimental data showed that the established separation efficiency and resistance model could accurately predict the separation and resistance performance of the dynamic pressure oil-air separator within a certain range; the average error of the four separation characteristic prediction models was 3.5%, and the maximum error was less than 16%. The model that was established by the least square method had the highest accuracy; the average error of the multivariate nonlinear fitting of the four resistance characteristic prediction models was less than 4%, and the maximum error was less than 15%, which could be used to predict the resistance performance of the separator. The applicable working condition of the model is lubricating oil flow rate 4.3~8.5 L/min and oil-air ratio 0.5~3.

1. Introduction

The phenomenon of gas-liquid separation exists widely in various industrial production fields, from biopharmaceutical and petroleum exploitation to aerospace. Especially in the field of aerospace, the engine requires a high performance lubrication system to ensure its safe and smooth operation in a high temperature, high pressure, and high speed working environment. Due to the overall requirements of the engine's small size and light weight, the design requirements for each element of the lubrication system have become more strict. During the operation of the engine, clean and low-temperature lubricating oil is transferred to the rotating parts of the engine, thus reducing friction and taking away the heat generated by friction. Air will enter the lubrication system due to the difference in pressure between the inside and outside. Under the action of high-speed rotating parts, the lubricating oil is mixed with air to form lubricating oil emulsion, which is transferred to the oil return system by the oil return pump. In order to ensure the safe operation of the engine, the design capacity of the oil return pump is often greater than the oil supply, and it will also send a large amount of air to the oil return system when working. Therefore, the fluid in the oil return system is a two-phase mixture of oil and air, which will increase pipeline resistance, reduce the performance of the oil-burning radiator, and affect the lubrication conditions of the counterface under the friction. In addition, if the two-phase mixture of oil and air enters directly into the oil supply system, it will cause the decrease in oil supply pressure and oil supply, thus seriously affecting the safety of the engine. Therefore, it is necessary to install an oil-air separation device in the oil return system. Due to the advantages of its simple structure and lightweight, the dynamic pressure oil-air separator has been widely used in small aeroengines [1], but its flow field is more complicated, involving anisotropic three-dimensional rotating flow, and there are a large number of local secondary flows, such as central return flow, local circulation flow, local short circuit flow, and other flow phenomena. At the same time, due to the existence of the two-phase mixture of oil and air, the flow field also has a

complex change of the two-phase interface. All these factors all increase the difficulty of the separator design and optimization process.

In recent years, the researches on dynamic pressure oil-air separation has mainly focused on the Gas-Liquid Cylindrical Cyclone (GLCC), discussing the flow characteristics and mechanical behavior of the separator. In terms of experimental research, Gomez et al. [2] tested the distribution of the subvelocity field in the separator and the changes of the turbulence related quantities at different positions of the separator. Hreiz et al. [3, 4] conducted in-depth experiments on the swirl characteristics of the internal flow field of the tubular gas-liquid separator and discussed the influence of the inlet shape on the flow field and working performance and proved that the rectangular tapered inlet could effectively improve the performance of the separator. Hsiao et al. [5] discussed the influence of the inlet form on the flow field of the separator and found that the change of the inlet form directly affected the internal flow pattern of the separator, thus affecting the separation efficiency of the separator. Fan et al. [6] used PIV to measure the internal flow field of the separator. By comparing the axial velocity, radial velocity, and separation efficiency, they discussed the influence of different inlet angles on the separator. With the rapid development of computer technology, numerical simulation methods have been widely used in the research of separators. Reyes-Gutiérrez et al. [7, 8] analyzed the single-phase and two-phase flow fields in the separator and discussed the influence of flow and structure parameters on the separation performance. The results showed that the separation efficiency was greatly affected by the behavior of the separator gas core. The installation of the annular membrane device could effectively improve the separation efficiency of GLCC. Yang [9] et al. established the bubble motion trajectory equation from a theoretical perspective and studied the mechanical behavior of the bubble in the separator. In addition, Lu and Hu [10] used the DPM model to study the movement of oil droplets in the cyclone separator and calculated the oil droplet size distribution using a semiempirical formula. The results showed that the splashing phenomenon of oil droplets in the separator would cause the separation performance to decline. On this basis, considering the effect of the dynamic contact angle of the spatial interface, Alinejad and Peiravi [11] studied the phenomenon of collision and fracture between two cylinders in nine different modes and made quantitative and qualitative analysis with the experimental results. Guizani et al. [12] simulated the velocity field distribution in the separator by combining the RSM model and the DPM model, and the simulation results well reflected distribution law of the flow field. Van [13] used RSM to discuss the effect of the inlet angle on the single-phase flow field in the separator and presented the difference of the flow field distribution in different situations and the improved design of the separator structure. Wang et al. [14] also used RSM to simulate the cyclone field in the separator and obtained the pressure drop and velocity distribution rules of the flow field in the separator. The simulation results were consistent with the experimental results. On this basis, Zhu et al. [15] studied the outlet forms at the bottom of the separator by using RSM and discussed the influence of different outlet forms on the flow field distribution. They believed that the single tangential outlet is more conducive to improving the separation efficiency. Ghasemi et al. [16] conducted a numerical simulation of the separator using the Eulerian model and discussed the influence of structural factors such as inlet width, inlet angle, inlet height, cylinder diameter, and outlet pipe diameter on the separation efficiency and proposed a structural optimization scheme.

As a numerical method that can truly reflect the interaction between fluid particles and improve the calculation accuracy of the flow field, LBM (Lattice Boltzmann method) is widely used in the field of flow and optimization [17, 18]. It has the potential to describe the local secondary flow phenomenon of the flow field. Derksen and Van [19, 20] used the LBM method to study the gas phase swirling flow field of cyclone separator and accurately described the phenomenon of precession vortex core (PVC) at the vortex center of the gas phase flow field. Hu et al. [21] also used the D3Q9 model in LBM to simulate the single-phase cyclone field in the hydrocyclone. They found that the simulation result of the secondary reflux of the center was better than that of Hreiz et al. [22]. Meanwhile, the simulation also captured the unsteady characteristics of the vortex core in the flow field.

Berrio et al. [23] studied the influence of inlet angle, position, quantity, shape, and other factors on liquid entrapment at the gas outlet of separator and gave the optimal value within the scope of the research. Venkatesh et al. [24] optimized the structure of the separator through the Taguchi method, conducted a simulation study on the separation efficiency through RSM and DPM, and found that the performance of the modified separator was improved. Wasilewski and Brar [25] used RSM and DPM to study the inlet structures of twenty different separators and found that curved inlet had little influence on separation efficiency, but greater influence on Eu number. Li et al. [26] used the PBM model to conduct numerical simulate of the flow field in the agitator and compared the simulation results of five different droplet breaking models on the droplet breaking process. Siadaty and Huang et al. [27, 28] used the Eulerian-Lagrange method to conduct a comprehensive study on the effects of airflow and structure on the performance of cyclones. The analysis results showed that the higher the temperature, the weaker the swirling flow, and the flow pressure drop and particle separation efficiency were significantly reduced. At the same time, increasing the air gap width and reducing the exhaust angle of the guide vane could improve the separation efficiency. Li et al. [29] took the axial cyclone separator with an inner diameter of 150 mm as the research object and studied the influence of material humidity on its inlet particle size distribution, overall efficiency, classification efficiency, and cutting particle size. It was found that when the inlet velocity and the particle humidity were constant, due to the aggregation of the particles, as the particle concentration increases, the efficiency of both the collection and classification were significantly improved. Wang et al. [30] studied the separation process of oil droplets in the swirling flow. Based on the numerical simulation and the experimental results, they

established a numerical model for the impact of the collision and breakup of the droplets to the separation efficiency on the wall. Yue et al. [31] used experiments and numerical simulations to explain the flow state and flow behavior of the upper spinning liquid film (USLF) in the gas-liquid cylindrical cyclone. Based on the experiments, the four flow patterns were determined, which were swirling flow, stirring flow, annular flow, and ribbon flow, and their flow pattern diagrams were also established. Yang et al. [32] also combined experiments and numerical analysis in the study of the separation characteristics of the gas-liquid cylindrical cyclone. The results showed that a separator with a strong swirling flow might not be able to achieve a better separation result. Finally, based on the force of the droplet and the swirling dynamics, a droplet migration model was established and accurately predicted the separation performance of the droplet.

Generally speaking, most of the past researches are mainly focused on hydrocyclone separators in industrial fields such as petrochemicals and bioengineering. However, due to factors such as small inlet flow and limited installation space, the structural dimensions of aeroengine hydrocyclone separators are quite different. This results in differences in the flow field of the separator, and the influence of the structure on the flow field will also change. Therefore, the research results on the hydrocyclones are difficult to be applied directly to the aerospace field. Although, in speaking of the separators exclusively for aeroengine, experimental research is the most direct method, it is difficult to obtain sufficient and complete experimental data. Moreover, if the characteristics of the separator are analyzed directly from the perspective of theory and mechanism, many influencing factors need to be overlooked. Most of the established models are semiempirical formulas, which have certain errors and are not universal. Although the semianalytical solution methods such as AGM (Akbari-Ganji's method) [33–35] and HAM (homotopy analysis method) [36] can directly obtain more accurate linear or nonlinear solutions, the difficulty of its application is relatively large, which is not conducive in solving practical engineering problems. Numerical simulations can clearly present the flow conditions inside the separator, and most of the physical models proposed by the current research are not perfect due to the lack of an overall description of the relevant characteristics of the separator. Hence, the three methods are difficult to establish a mathematical model representing the performance of the separator as a whole.

Therefore, this paper adopts the dimensional analysis method and combines with the experimental data of the separator to establish the prediction model of the dynamic pressure oil-air separator's characteristics based on the main physical parameters affecting the performance of the separator. According to the simulation data, the performance prediction model of the separator is optimized and improved. The prediction model can effectively predict the separation efficiency and resistance performance of the separator after the error test analysis and model verification, so as to provide a reference for the design and improvement of the separator.

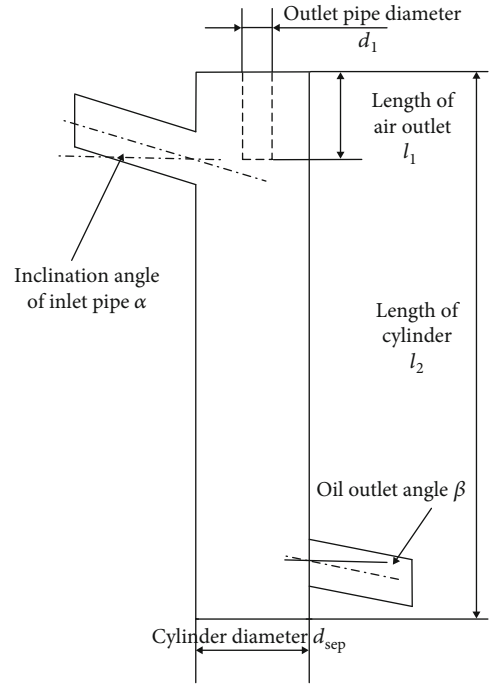

Figure 1: Separator structure diagram.

2. Predictive Model

2.1. Flow and Structural Parameters. A large number of scholars have studied the influence of flow rate, oil-air ratio, and structural parameters on the performance of separators. At the same time, they also put forward suggestions for improving of the structural parameters of the separators. However, the dynamic pressure types of oil-air separators for aeroengine are quite different, and the research results are relatively few. The parameters that affect the performance of the dynamic pressure oil-air separator mainly include the working condition parameters and the structural parameters. The working condition parameters refer to the state of the internal medium of the separator during operation. The structural parameters are the structural dimensions of the components constituting the separator. Together, they determine the performance of the separator. The definition of the structure parameters of the separator is shown in Figure 1, and the values of the structure and working condition parameters are shown in Table 1.

2.2. Predictive Model Establishment. The separator performance prediction model established in this paper includes the following parameters. These parameters and dimensions are listed in Table 2. The flow rate is replaced by the flow rate at the inlet; in addition, the mixture density and lubricating oil density are used to describe the state of the two-phase mixture.

2.2.1. Establishment of the Separation Efficiency Prediction Model. After determining the factors affecting the performance of the separator, the core physical quantities need to be selected. In this paper, d_{sep}, ρ, and v are selected as the core

Table 1: Condition and structure parameter values.

Name		Parameter value						
Working condition parameters	Flow q_l/(L/min)	4.3	5	6*	7	8	8.5	—
	Oil-air ratio ε	0.5	1*	1.5	2	2.5	3	—
	Lubricating oil temperature T/(°C)	30	50	80	100	150	200*	—
Structural parameters	Length of cylinder l_2/mm	60	70	80	90*	100	110	120
	Cylinder diameter d_{sep}/mm	10	12	14	16*	18	20	—
	Length of air outlet l_1/mm	0	5	10	15*	20	25	—
	Outlet pipe diameter d_1/mm	2	3*	4	5	6	7	8
	Entrance angle α /°	0	5°	10°	15°*	20°	25°	—
	Inclination angle of the outlet pipe β /°	0°*	5°	10°	15°	20°	25°	—

Table 2: Main influence parameters and dimensions.

Name	Length of air outlet	Length of cylinder	Outlet pipe diameter	Cylinder diameter	Oil outlet pipe angle	Angle of inlet pipe
Symbol	l_1	l_2	d_1	d_{sep}	β	α
Unit	m	m	m	m	°	°
Dimension	L	L	L	L	—	—
Name	Inlet flow rate	Oil viscosity	Oil-air ratio	Mixture density	Oil density	
Symbol	v	μ	ε	ρ	ρ_y	
Unit	m/s	Pa·s	—	Kg/m^3	Kg/m^3	
Dimension	L·T^{-1}	M·L^{-1}·T^{-1}	—	M·L^{-3}	M·L^{-3}	

physical quantities of the separation characteristic prediction model, and the dimensionless equation is established as [37]

$$F\left(l_1, l_2, d_1, d_{sep}, \beta, \alpha, v, \mu, \varepsilon, \rho, \rho_y, \eta\right) = 0. \quad (1)$$

The function of the physical process in the separator is constructed by the dimensional analysis method. It is known that when processing the results of experiments or numerical simulations, it is usually used in the range of $(\pi_1,\pi_2,\ldots,\pi_{n-3})$ to arrange the results into a power law relationship [38]. Use π theorem to get its criterion equation:

$$\begin{cases} \pi_1 = \dfrac{l_1}{{d_{sep}}^{a_1}\rho^{b_1}v^{c_1}} & \pi_2 = \dfrac{l_2}{{d_{sep}}^{a_2}\rho^{b_2}v^{c_2}} & \pi_3 = \dfrac{d_1}{{d_{sep}}^{a_3}\rho^{b_3}v^{c_3}}, \\ \pi_4 = \dfrac{\rho_y}{{d_{sep}}^{a_4}\rho^{b_4}v^{c_4}} & \pi_5 = \dfrac{\mu}{{d_{sep}}^{a_5}\rho^{b_5}v^{c_5}} & \pi_6 = \beta, \\ \pi_7 = \alpha & \pi_8 = \varepsilon & \pi_9 = \eta. \end{cases} \quad (2)$$

According to the principle of dimensional consistency, the index determination method of each item is

$$\begin{cases} \mathrm{L} = \mathrm{L}^{a_1}\left(\mathrm{ML}^{-3}\right)^{b_1}\left(\mathrm{LT}^{-1}\right)^{c_1}, \\ \mathrm{L} = \mathrm{L}^{a_2}\left(\mathrm{ML}^{-3}\right)^{b_2}\left(\mathrm{LT}^{-1}\right)^{c_2}, \\ \mathrm{L} = \mathrm{L}^{a_3}\left(\mathrm{ML}^{-3}\right)^{b_3}\left(\mathrm{LT}^{-1}\right)^{c_3}, \\ \mathrm{ML}^{-3} = \mathrm{L}^{a_4}\left(\mathrm{ML}^{-3}\right)^{b_4}\left(\mathrm{LT}^{-1}\right)^{c_4}, \\ \mathrm{ML}^{-1}\mathrm{T}^{-1} = \mathrm{L}^{a_5}\left(\mathrm{ML}^{-3}\right)^{b_5}\left(\mathrm{LT}^{-1}\right)^{c_5}. \end{cases} \quad (3)$$

The coefficients can be obtained by using formula (3), and the coefficients can be brought into formula (2) to obtain

$$\begin{cases} \pi_1 = \dfrac{l_1}{d_{sep}} & \pi_2 = \dfrac{l_2}{d_{sep}}, \\ \pi_3 = \dfrac{d_1}{d_{sep}} & \pi_4 = \dfrac{\rho_y}{\rho}, \\ \pi_5 = \dfrac{\mu}{d_{sep}\rho v} = \dfrac{1}{\mathrm{Re}} & \pi_6 = \beta, \\ \pi_7 = \alpha, \pi_8 = \varepsilon & \pi_9 = \eta. \end{cases} \quad (4)$$

The separation efficiency prediction model:

$$\eta = K\left(\frac{l_1}{d_{sep}}\right)^{\beta_1}\left(\frac{l_2}{d_{sep}}\right)^{\beta_2}\left(\frac{d_1}{d_{sep}}\right)^{\beta_3}\left(\frac{\rho_y}{\rho}\right)^{\beta_4}\left(\frac{1}{\mathrm{Re}}\right)^{\beta_5}\beta^{\beta_6}\alpha^{\beta_7}\varepsilon^{\beta_8}. \tag{5}$$

Take the logarithm of the left and right sides of equation (5) to convert the nonlinear model into a linear model. Take the logarithm of the left and right sides of equation (5) and use the 492 sets of separation efficiency and resistance data obtained in experiment [39] to process them by the least square method. The result is shown in equation (6). At the same time, the forward selection method, the backward selection method, and the stepwise selection method [40–43] are used to delete and select variables to simplify the model form. The results are shown in equations (7)–(9).

$$\eta = e^{3.04436}\left(\frac{l_1}{d_{sep}}\right)^{-0.01313}\left(\frac{l_2}{d_{sep}}\right)^{-0.07590}\left(\frac{d_1}{d_{sep}}\right)^{0.07744}\left(\frac{\rho_y}{\rho}\right)^{-0.11899}\left(\frac{1}{\mathrm{Re}}\right)^{-0.11335}\beta^{0.00571}\alpha^{0.01305}\varepsilon^{0.00845}, \tag{6}$$

$$\eta = e^{2.87668}\left(\frac{d_1}{d_{sep}}\right)^{0.06055}\left(\frac{\rho_y}{\rho}\right)^{-0.13159}\left(\frac{1}{\mathrm{Re}}\right)^{-0.11607}, \tag{7}$$

$$\eta = e^{3.00342}\left(\frac{l_2}{d_{sep}}\right)^{-0.08098}\left(\frac{d_1}{d_{sep}}\right)^{0.06918}\left(\frac{\rho_y}{\rho}\right)^{-0.13}\left(\frac{1}{\mathrm{Re}}\right)^{-0.11546}\alpha^{0.01402}, \tag{8}$$

$$\eta = e^{3.05709}\left(\frac{l_1}{d_{sep}}\right)^{-0.01308}\left(\frac{l_2}{d_{sep}}\right)^{-0.07590}\left(\frac{d_1}{d_{sep}}\right)^{0.07725}\left(\frac{\rho_y}{\rho}\right)^{-0.13846}\cdot\left(\frac{1}{\mathrm{Re}}\right)^{-0.11337}\beta^{0.00568}\alpha^{0.01308}. \tag{9}$$

2.2.2. Establishment of the Resistance Prediction Model. According to the same methods and steps as the separation efficiency model, the resistance prediction model can be established, and the result is

$$\frac{\Delta P}{\rho v^2} = K^*\left(\frac{l_1}{d_{sep}}\right)^{\theta_1}\left(\frac{l_2}{d_{sep}}\right)^{\theta_2}\left(\frac{d_1}{d_{sep}}\right)^{\theta_3}\left(\frac{\rho_y}{\rho}\right)^{\theta_4}\left(\frac{\mu}{d_{sep}\rho v}\right)^{\theta_5}\beta^{\theta_6}\alpha^{\theta_7}\varepsilon^{\theta_8}. \tag{10}$$

Equation (10) is processed with the equal sign, and the result is shown in equations (11)–(13). The expression of the stepwise selection method and backward selection method is the same, see equation (13).

Table 3: Separation efficiency model verification.

Model	F statistics	F critical value	Probability	R^2
Least squares method	19.99	2.143	<0.0001	0.7766
Forward selection	23.34	2.207	<0.0001	0.7766
Backward selection	49.38	2.783	<0.0001	0.7439
Step by step selection	32.19	2.400	<0.0001	0.7666

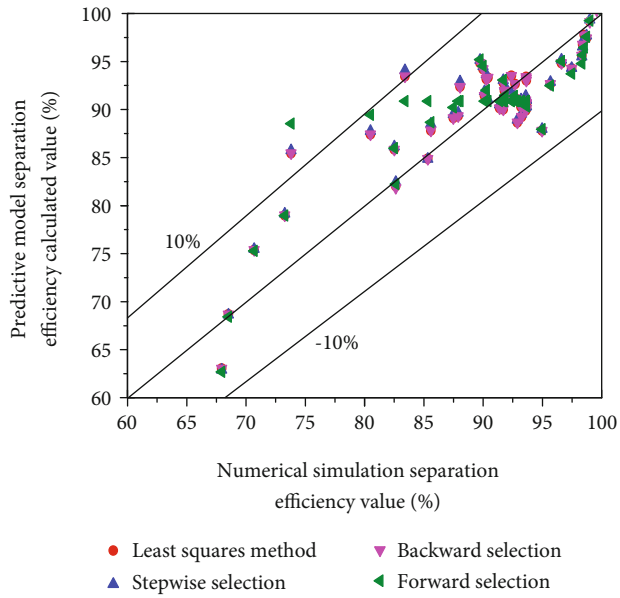

Figure 2: Error comparison of the separation efficiency model.

Table 4: Error analysis of the separation efficiency model.

	Least squares method	Step by step selection	Backward selection	Forward selection
Average error/%	2.12	2.21	2.22	2.36
Maximum error/%	10.7	12.3	14.7	15.9

$$\frac{\Delta P}{\rho v^2} = e^{1.54768}\left(\frac{l_1}{d_{sep}}\right)^{0.03249}\left(\frac{l_2}{d_{sep}}\right)^{0.37875}\left(\frac{d_1}{d_{sep}}\right)^{-0.54378}\left(\frac{\rho_y}{\rho}\right)^{3.43402}\left(\frac{\mu}{d_{sep}\rho v}\right)^{0.33546}\beta^{-0.0003295}\alpha^{-0.02269}\varepsilon^{2.04374} \tag{11}$$

Table 5: Resistance model verification.

Model	F statistics	F critical value	Probability	R^2
Least squares method	149.74	2.143	<0.0001	0.9630
Stepwise selection (forward selection)	174.84	2.138	<0.0001	0.9630
Backward selection	199.51	2.203	<0.0001	0.9614

$$\frac{\Delta P}{\rho v^2} = e^{1.54877}\left(\frac{l_1}{d_{sep}}\right)^{0.0324}\left(\frac{l_2}{d_{sep}}\right)^{0.37873}\left(\frac{d_1}{d_{sep}}\right)^{-0.54345} \cdot \left(\frac{\rho_y}{\rho}\right)^{3.43641}\left(\frac{\mu}{d_{sep}\rho v}\right)^{0.33556}\alpha^{-0.02273}\varepsilon^{2.04495}, \tag{12}$$

$$\frac{\Delta P}{\rho v^2} = e^{1.53832}\left(\frac{l_2}{d_{sep}}\right)^{0.39366}\left(\frac{d_1}{d_{sep}}\right)^{-0.53522}\left(\frac{\rho_y}{\rho}\right)^{3.46} \cdot \left(\frac{\mu}{d_{sep}\rho v}\right)^{0.33688}\alpha^{-0.02323}\varepsilon^{2.05713}. \tag{13}$$

3. Predictive Model Test

The predictive model testing mainly includes two aspects: one is to test the reliability of the estimated parameters of the equation and the model using the mathematical statistical methods. The second is to analyze the errors in the fitting process of the predictive model.

3.1. Separation Efficiency Model Test. The significance test of each separation characteristic prediction model is performed, and the results are shown in Table 3. The F statistic value in the table is used to determine whether the calculated value of various prediction models can represent the true value. When the F statistic value is greater than the critical value, the prediction model is considered to reflect the true situation; R^2 is the correlation coefficient; the larger the value is, the stronger the correlation between the variable and the prediction model is [44].

As can be seen from Table 3, the correlation coefficient R^2 of the separation characteristic prediction model established by the four methods is about 0.75, so the dependent variable and the independent variable have a good correlation; at the 0.05 significance level, the F statistic value is greater than the critical value, F. The statistical probabilities are all less than 0.0001, indicating that the four prediction models of separation characteristics are highly significant.

Next, the fitting error of the prediction model is analyzed. Taking the separation efficiency obtained by numerical simulation in the literature [39] as the abscissa and the separation efficiency calculated by the prediction model as the ordinate, the separation efficiency fitting error graph is drawn, as shown in Figure 2. Table 4 shows the average error and maximum error of the four prediction models. In combination with Figure 2 and Table 4, it can be concluded that in the multivariate nonlinear fitting, the average error of the four models is less than 3.5%, and the maximum error is less than 16% (the maximum is 15.9%). According to the date from small to large, the four models are the least square method, backward selection method, forward selection method, and stepwise selection method. This indicates that the prediction model with stronger significance has higher accuracy and smaller relative error, but contains more variables, such as the model obtained by the least square method. The backward selection method is the opposite, and the model established has the lowest precision but the least variables, which makes the engineering application more convenient. Comparing the variables in equations (6)–(9), it can be found that the stepwise selection method, forward selection method, and backward selection method all remove the effect of ε on the separation efficiency, but the oil-air ratio ε cannot be ignored in practical engineering applications. Hence, the three models will not be discussed in the following research.

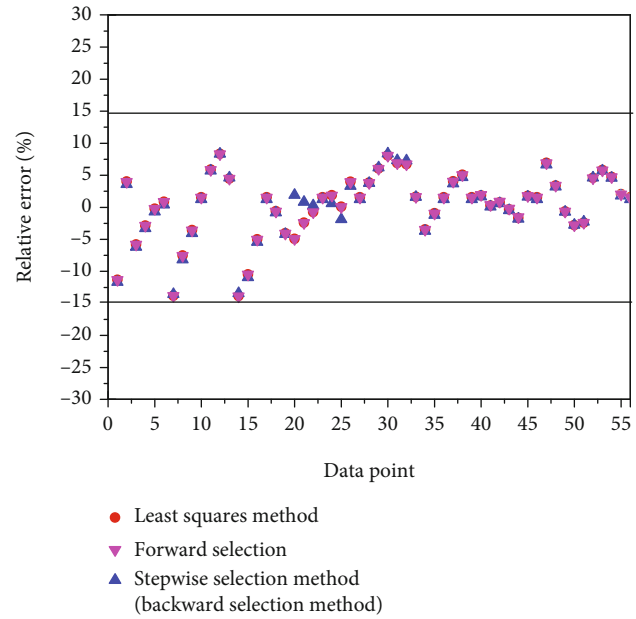

Figure 3: Error comparison of the resistance model.

Table 6: Error analysis of the resistance model.

	Least squares method	Stepwise selection (backward selection method)	Forward selection
Average error/%	3.93	3.87	3.93
Maximum error/%	13.8	13.9	13.8

3.2. Resistance Model Testing. The significance test of each resistance characteristic prediction model is carried out, and the results are shown in Table 5. It can be seen from Table 5 that at the 0.05 significance level, the F statistic value of the established resistance characteristic prediction model is large and much larger than the critical value, the F statistic probability is less than 0.0001, and the correlation coefficient R^2 is close to 1. Therefore, the dependent variable and the independent variable are significantly correlated, and the significance is high, which meets the standard of the significance test.

Next, the fitting error of the prediction model is analyzed. Since the resistance value of the separator is between 400 Pa and 2800 Pa under different working conditions, the distribution interval is large, so the form of Figure 2 is not suitable. Here, only the relative errors under different working conditions are drawn, as shown in Figure 3; the error analysis is shown in Table 6. Combining Figure 3 and Table 6, it can be concluded that the average error of the four models is low, less than 4%, and the maximum error is less than 15% (the maximum is 13.9%); the overall errors of the four prediction models are very close, so it is difficult to evaluate its pros and cons. Comparing the variables in equations (11)–(13), the forward selection method removes the influence of β, and the stepwise selection method (backward selection method) removes the influence of β and l1. β and l1 have little influence on resistance. It indirectly shows that β and l1 are not strongly related to separator resistance, so the four models established in this paper are suitable for the prediction of the separator resistance performance.

4. Application of Predictive Models

According to the analysis of the multivariate nonlinear fitting error of the separator performance prediction model, it can be seen that each model has passed the significance test, indicating that it can be used for the prediction of separator performance. In this section, we will combine the obtained experimental data to further test the accuracy of the prediction model.

4.1. Separation Efficiency Prediction. It can be seen from the foregoing that after the elimination of variables, the prediction model of separation efficiency cannot reflect the effect of ε on the performance of the separator, so this section will only discuss the prediction model established by the least square method. Substituting the flow and structural parameters of the dynamic pressure type oil-air separator into equation (9), the efficiency value of the separator under each experimental working condition is calculated and compared with the experimental value. The results are shown in Figures 4–7. Figures 4–7 show the comparison between the separation efficiency calculated by the prediction model and the experimental data under the conditions of different cylinder diameters, inlet inclination angles, outlet pipe diameters, and outlet pipe lengths. It can be seen from Figure 4–6 that the separation efficiency calculated by the prediction model is close to the experimental value, and the overall trend distribution is consistent; that is, as the flow rate increases, the separation efficiency gradually decreases; as the diameter of the outlet pipe increases, the separation efficiency gradually increases. It can be seen from Figure 7 that the difference between the calculated value of the prediction model and the experimental value is small, but the experimental data in the figure shows the maximum separation efficiency at $l_1/l_2 = 0.19$, while the prediction model does not show this phenomenon. The separation efficiency prediction model equation is in exponential form, see formula (9). When discussing the influence of a certain factor, there will be a monotonic increase or decrease in separation efficiency; that is, the prediction model cannot obtain the optimal separator

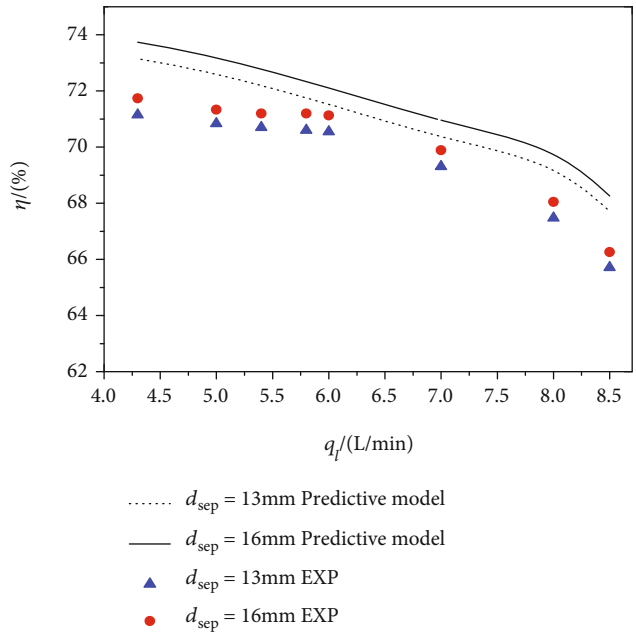

Figure 4: Comparison of separation efficiency at different cylinder diameters.

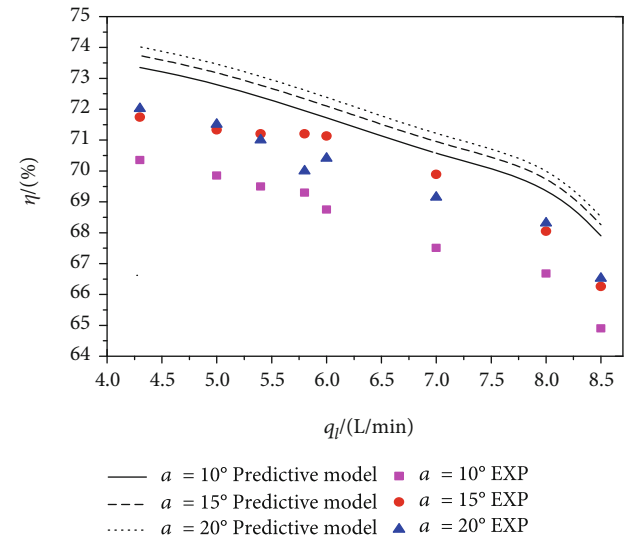

Figure 5: Comparison of separation efficiency at different inlet inclination angles.

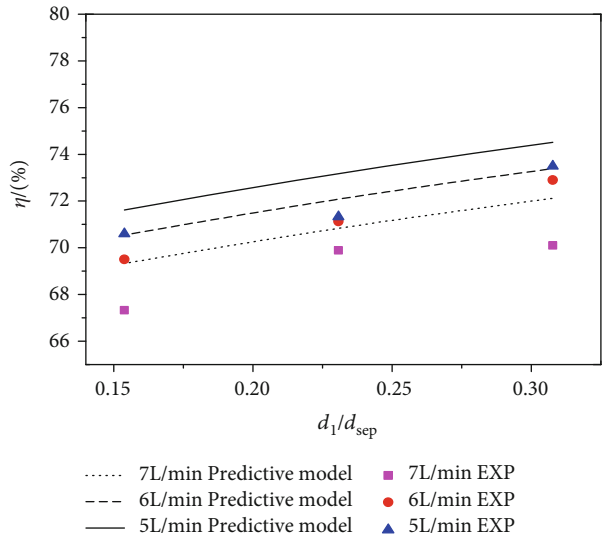

Figure 6: Comparison of separation efficiency at different outlet trachea diameters.

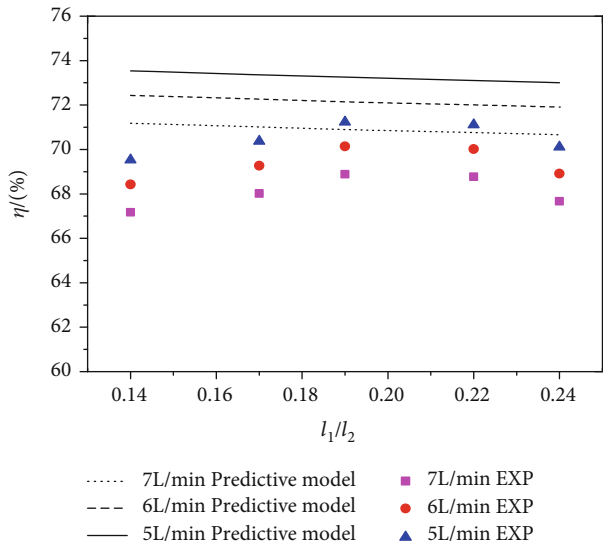

Figure 7: Comparison of separation efficiency at different outlet trachea lengths.

structure size. This is a flaw in the model, which is currently being reviewed for improvement.

In addition, it can be seen from Figures 4–7 that under the same conditions, the calculated value of the prediction model is greater than the experimental value. The analysis believes that during the experiment, it takes a certain amount of time from the beginning of the oil sample collection to the end of the collection. During this period of time, the oil sinks due to gravity, and the gas rises and leaves the collection device. The volume of this part of the gas cannot be included in the calculation of the separation efficiency. As a result, the measured value of the separation efficiency is relatively small. Therefore, this article believes that the above phenomenon is reasonable.

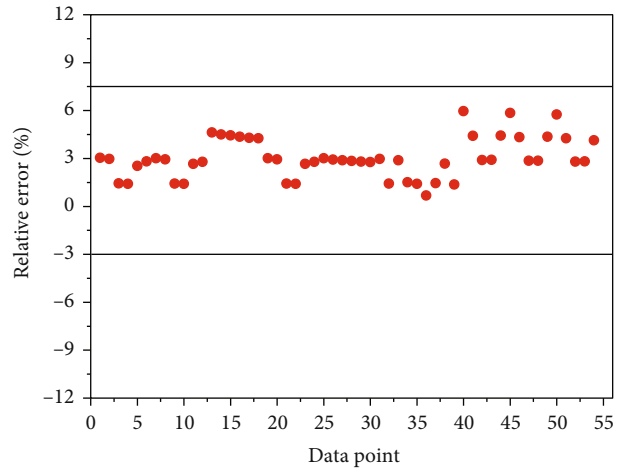

Figure 8: Error of the prediction model and experimental data.

In order to further analyze the accuracy of the prediction model, 54 sets of experimental data obtained from the experiment were used to analyze the overall error, and the result is shown in Figure 8. It can be seen from the figure that the calculation error of the prediction model under each working condition is small, with the maximum error is 6%, and the average error is 3.03%. In summary, the prediction model established in this paper can effectively predict the separation performance of the separator.

4.2. Resistance Prediction. Comparing equations (11)–(13), it can be seen that the number of variables in the resistance prediction model established by the four methods differs by 1~2, and the index of each variable is almost the same. Therefore, this section only will only discuss the resistance prediction model established by the least square method. Moreover, in the process of research on the performance of the separator, due to the severe fluctuation of the pressure of the two-phase mixture, the accurate value of the separator resistance cannot be obtained. Therefore, in this section, the numerical simulation data obtained from the literature [19] will be used to examine the resistance prediction model. According to the analysis in Section 3, the average error of the four resistance prediction models established in this paper is relatively small, which is suitable for the prediction of separator performance. However, whether it can predict the influence of flow and structural parameters on the performance of the separator is not clear, so this section focuses on this issue, as shown in Figure 9. It can be seen from the figure that with the increase of flow rate, oil-air ratio, and cylinder length and the decrease of temperature, cylinder diameter, and inlet inclination angle, the resistance of the separator increases, and the resistance distribution curve obtained by the prediction model is consistent with the trend of CFD data, indicating that the resistance model can well predict the influence of the six parameters. In Figure 9(f), it can be seen that the resistance distribution calculated by CFD is shape like a "snake", but the prediction model is monotonically increasing. In addition, Figure 9(h) shows that the curve obtained by the resistance prediction model is flat. With the increase of the

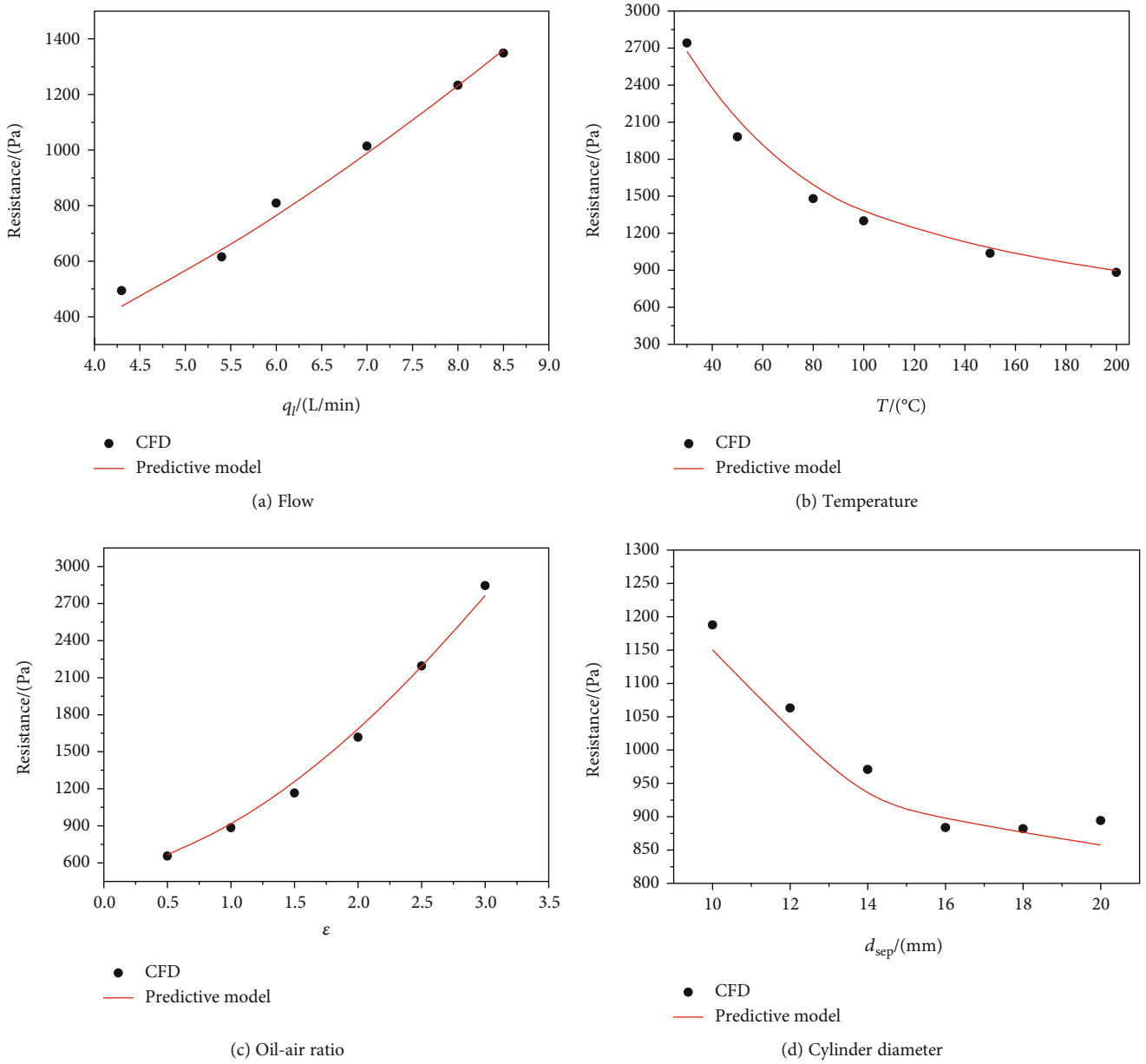

Figure 9: Continued.

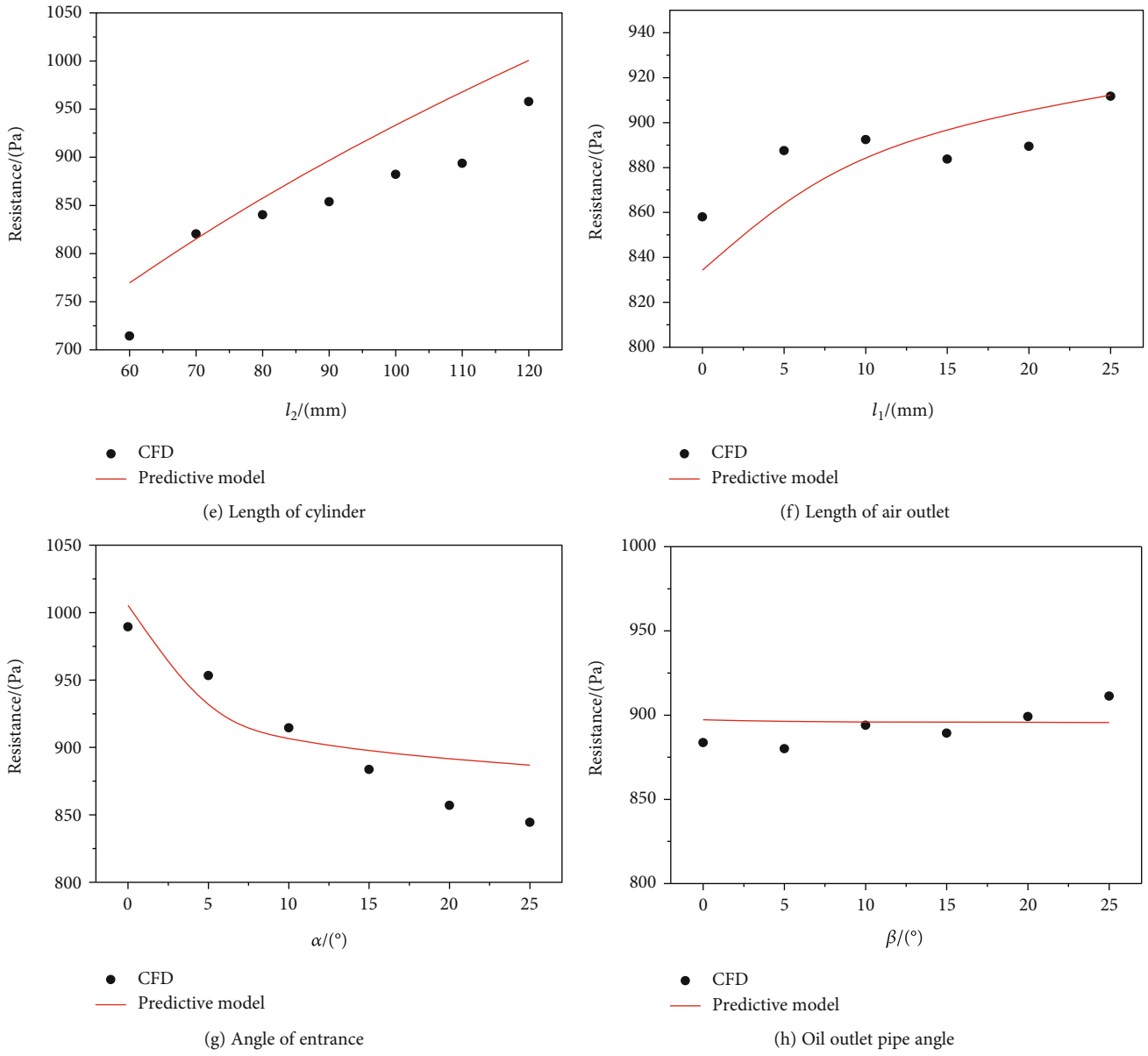

Figure 9: Effect of flow and structure parameters on separator resistance.

outlet pipe angle, the resistance decreases slightly, and the trend obtained by the numerical simulation increases slightly. However, the analysis of the resistance data shows that β is when the distribution is $0 \sim 25^{\circ}$, the resistance in the separator is between 880 Pa and 920 Pa. In view of the fact that this paper uses 11 kinds of parameter multivariate nonlinear fitting to establish the resistance prediction model, the error is acceptable.

From the above analysis, it can be seen that when using the predictive model to study the internal resistance of the separator, the calculated value and the numerical simulation result not only consistent in trend but also the value is almost identical. In an in-depth analysis of the accuracy of the resistance prediction model, the analysis of the overall error was conducted between the predicted value of the resistance model and the CFD simulation value. The results are shown in Figure 10. As seen in Figure 10, the calculation error of the prediction model under each working condition is relatively small, with the maximum error being 11.36% and the average error being 3.13%. Therefore, it is believed that the resistance prediction model established in this paper can effectively predict the resistance performance of the separator.

In summary, the applicable scope of the separation efficiency and resistance prediction model can be summarized: $q_l \in$ [4.3~8.5] L/min, $\varepsilon \in$ [0.5~3], $T \in$ [30~200] °C, $l_2 \in$ [60~120] mm, $d_{sep} \in$ [10~20] mm, $l_1 \in$ [0~25] mm, $d_1 \in$ [2~3] mm, $\alpha \in$ [0~25]°, and $\beta \in$ [0~25]°. Within this range, the model can effectively predict the separation efficiency and resistance of the separator.

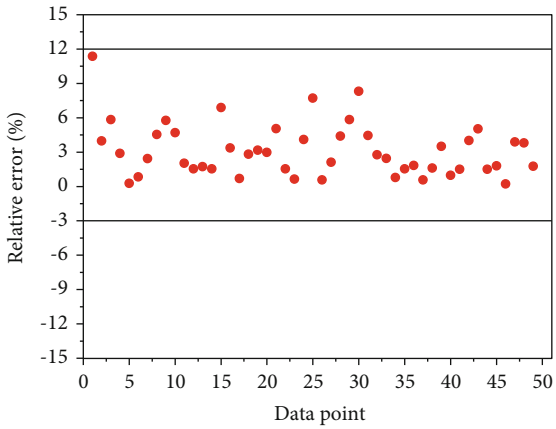

Figure 10: Error of the prediction model and simulation data.

5. Conclusion

This paper uses the principle of dimensional analysis to establish a prediction model for the separation characteristics and resistance characteristics of a dynamic pressure oil-air separator, analyzes the multiple nonlinear fitting errors, and compares with experimental data to verify the accuracy of the model. The conclusions are as follows:

(1) By using the principle of dimensional analysis, the prediction model of the separation and resistance characteristics of the dynamic pressure oil-air separator with sufficient accuracy can be established. In addition, the dependent variables and independent variables have a good correlation and a high significance for the established prediction model of separation and resistance characteristics, which conforms to the significance test standard

(2) As the flow rate increases, the separation efficiency gradually decreases; as the diameter of the outlet pipe increases, the separation efficiency gradually increases; the maximum separation efficiency appeared at $l_1/l_2 = 0.19$. With the increase of the flow rate, oil-air ratio, and cylinder length and the decrease of temperature, cylinder diameter, and inlet inclination angle, the resistance of the separator increases

(3) The average error of the multivariate nonlinear fitting of the four separation characteristic prediction models is less than 3.5%, and the maximum error is less than 16%. From small to large, the four models are the least square method, backward selection method, forward selection method, and stepwise selection method. The average error compared with the experimental data is less than 3.03%, and the maximum error is less than 6%. The model that is established by the least square method can accurately predict the separation efficiency of the separator under various working conditions

(4) The average error of the multivariate nonlinear fitting of the four resistance characteristic prediction models is less than 4%, and the maximum error is less than 15%. The overall error of the four prediction models is very close, which can be used to predict the resistance performance of the separator. The calculation error of the prediction model in each working condition is small, the average error between the model and the simulated value is 3.13%, and the maximum error is 11.36%. Therefore, it is considered that the resistance prediction model established in this paper can effectively predict the resistance performance of the separator

(5) The model built in this article can be used: $q_l \in$ [4.3~8.5] L/min, $\varepsilon \in$ [0.5~3], $T \in$ [30~200] °C, $l_2 \in$ [60~120] mm, $d_{sep} \in$ [10~20]mm, $l_1 \in$ [0~25]mm, $d_1 \in$ [2~3]mm, $\alpha \in$ [0~25]°, and $\beta \in$[0~25]° as performance prediction of dynamic pressure oil-air separator within the scope.

Data Availability

All data generated or analyzed during this study are included in this article.

Conflicts of Interest

The authors declare that they have no financial and personal relationship with other people or organizations that can inappropriately influence their work. There is no professional or other personal interest of any nature or kind in any product, service, and company that could be construed as influencing the position presented in or the review of the paper.

References

[1] J. S. Lin, C. J. Chang, and J. G. Yang, *Aero engine design manual*, Navigate Industrical Press, Beijing, 2002.

[2] L. Gomez, R. Mohan, and O. Shoham, "Swirling gas-liquid two-phase flow-experiment and modeling part I: swirling flow Field," *Journal of Fluids Engineering*, vol. 126, no. 6, pp. 935–942, 2004.

[3] R. Hreiz, C. Gentric, N. Midoux, R. Lainé, and D. Fünfschilling, "Hydrodynamics and velocity measurements in gas–liquid swirling flows in cylindrical cyclones," *Chemical Engineering Research and Design*, vol. 92, no. 11, pp. 2231–2246, 2014.

[4] R. Hreiz, R. Lainé, J. Wu, C. Lemaitre, C. Gentric, and D. Fünfschilling, "On the effect of the nozzle design on the performances of gas–liquid cylindrical cyclone separators," *International Journal of Multiphase Flow*, vol. 58, pp. 15–26, 2014.

[5] T. C. Hsiao, S. H. Huang, C. W. Hsu, C. C. Chen, and P. K. Chang, "Effects of the geometric configuration on cyclone performance," *Journal of Aerosol Science*, vol. 86, pp. 1–12, 2015.

[6] Y. Fan, J. Wang, Z. Bai, J. Wang, and H. Wang, "Experimental investigation of various inlet section angles in mini-hydrocyclones using particle imaging velocimetry," *Separation and Purification Technology*, vol. 149, pp. 156–164, 2015.

[7] M. A. Reyes-Gutiérrez, L. R. Rojas-Solórzano, J. C. Marín-moreno, A. J. Meléndez-Ramírez, and J. Colmenares, "Eulerian-eulerian modeling of disperse two-phase flow in a gas-liquid cylindrical cyclone," *Journal of Fluid Engineering*, vol. 128, no. 4, pp. 832–837, 2006.

[8] M. F. Kang, N. C. Hoyt, J. Kadambi, and Y. Kamotani, "Study of gas core behavior of passive cyclonic two-phase separator for microgravity Applications," *Microgravity Science and Technology*, vol. 26, no. 3, pp. 147–157, 2014.

[9] C. M. Yang, *Mechanism model research and numerical simulation on dynamic pressure type gas-oil separator*, Harbin Engineering University, Harbin, 2013.

[10] Y. G. Lu and J. P. Hu, "Numerical simulation for air/oil separator of aero-engine," *Applied Mechanics and Materials*, vol. 510, pp. 197–201, 2014.

[11] J. Alinejad and M. M. Peiravi, "Numerical analysis of secondary droplets characteristics due to drop impacting on 3D cylinders considering dynamic contact angle," *Meccanica*, vol. 55, no. 10, pp. 1975–2002, 2020.

[12] R. Guizani, I. Mokni, H. Mhiri, and P. Bournot, "CFD modeling and analysis of the fish-hook effect on the rotor separator's efficiency," *Powder Technology*, vol. 264, pp. 149–157, 2014.

[13] S. L. Van, "Influence of inlet angle on flow pattern and performance of gas-liquid cylindrical cyclone separator," *Particulate Science and Technology*, vol. 35, pp. 555–564, 2016.

[14] S. Y. Wang, H. L. Li, R. C. Wang, X. Wang, R. Tian, and Q. Sun, "Effect of the inlet angle on the performance of a cyclone separator using CFD-DEM," *Advanced Powder Technology*, vol. 30, no. 2, pp. 227–239, 2019.

[15] W. B. Zhu, L. Hu, and X. B. Zhang, "The effects of the lower outlet on the flow field of small gas–liquid cylindrical cyclone," *Proceedings of the Institution of Mechanical Engineers, Part C: Journal of Mechanical Engineering Science*, vol. 233, no. 4, pp. 1989–1996, 2018.

[16] A. Ghasemi, M. Shams, and M. M. Heyhat, "A numerical scheme for optimizing gas liquid cylindrical cyclone separator," *Proceedings of the Institution of Mechanical Engineers, Part E: Journal of Process Mechanical Engineering*, vol. 231, no. 4, pp. 1–13, 2016.

[17] M. M. Peiravi and J. Alinejad, "Hybrid conduction, convection and radiation heat transfer simulation in a channel with rectangular cylinder," *Journal of Thermal Analysis and Calorimetry*, vol. 140, no. 6, pp. 2733–2747, 2020.

[18] M. M. Peiravi, J. Alinejad, D. D. Ganji, and S. Maddah, "3D optimization of baffle arrangement in a multi-phase nanofluid natural convection based on numerical simulation," *International Journal of Numerical Methods for Heat & Fluid Flow*, vol. 30, no. 5, pp. 2583–2605, 2020.

[19] J. Derksen and D. A. H. Van, "Simulation of vortex core precession in a reverse-flow cyclone," *AICHE Journal*, vol. 46, no. 7, pp. 1317–1331, 2000.

[20] S. Pirker, C. Goniva, C. Kloss, S. Puttinger, J. Houben, and S. Schneiderbauer, "Application of a hybrid Lattice Boltzmann–finite volume turbulence model to cyclone short-cut flow," *Powder Technology*, vol. 235, pp. 572–580, 2013.

[21] L. Hu, W. B. Zhu, and X. B. Zhang, "Lattice Boltzmann simulation of swirling flow in hydrocyclone," *Journal of Harbin Engineering University*, vol. 38, no. 12, pp. 1864–1871, 2017.

[22] R. Hreiz, C. Gentric, and N. Midoux, "Numerical investigation of swirling flow in cylindrical cyclones," *Chemical Engineering Research and Design*, vol. 89, no. 12, pp. 2521–2539, 2011.

[23] J. C. Berrio, E. Pereyra, and N. Ratkovich, "Computational fluid dynamics modeling of gas–liquid cylindrical cyclones, geometrical analysis," *Journal of Energy Resources Technology*, vol. 140, no. 9, 2018.

[24] S. Venkatesh, M. Sakthivel, S. Sudhagar, and S. A. A. Daniel, "Modification of the cyclone separator geometry for improving the performance using Taguchi and CFD approach," *Particulate Science and Technology*, vol. 37, no. 7, pp. 799–808, 2018.

[25] M. Wasilewski and L. S. Brar, "Effect of the inlet duct angle on the performance of cyclone separators," *Separation and Purification Technology*, vol. 213, no. 15, pp. 19–33, 2019.

[26] D. Li, A. Buffo, W. Podgórska, D. L. Marchisio, and Z. Gao, "Investigation of droplet breakup in liquid-liquid dispersions by CFD-PBM simulations: the influence of the surfactant type," *Chinese Journal of Chemical Engineering*, vol. 10, pp. 1369–1380, 2017.

[27] M. Siadaty, S. Kheradmand, and F. Ghadiri, "Study of inlet temperature effect on single and double inlets cyclone performance," *Advanced Powder Technology*, vol. 28, no. 6, pp. 1459–1473, 2017.

[28] L. Huang, S. S. Deng, Z. Chen, J. Guan, and M. Chen, "Numerical analysis of a novel gas-liquid pre-separation cyclone," *Separation and Purification Technology*, vol. 194, pp. 470–479, 2018.

[29] Y. Li, G. L. Qin, Z. Y. Xiong, Y. Ji, and L. Fan, "The effect of particle humidity on separation efficiency for an axial cyclone separator," *Advanced Powder Technology*, vol. 30, no. 4, pp. 724–731, 2019.

[30] L. Wang, J. Feng, G. Xiang, and X. Peng, "Investigation on the oil–gas separation efficiency considering oil droplets breakup and collision in a swirling flow," *Chemical Engineering Research & Design*, vol. 117, pp. 394–400, 2017.

[31] T. Yue, J. Y. Chen, J. F. Song et al., "Experimental and numerical study of upper swirling liquid film (USLF) among gas-liquid cylindrical cyclones (GLCC)," *Chemical Engineering Journal*, vol. 358, pp. 806–820, 2019.

[32] L. L. Yang, J. Zhang, Y. Ma, J. Xu, and J. Wang, "Experimental and numerical study of separation characteristics in gas-liquid cylindrical cyclone," *Chemical Engineering Science*, vol. 214, p. 115362, 2020.

[33] M. R. Akbari, D. D. Ganji, A. K. Rostami, and M. Nimafar, "Solving nonlinear differential equation governing on the rigid beams on viscoelastic foundation by AGM," *Journal of Marine Science and Application*, vol. 14, no. 1, pp. 30–38, 2015.

[34] H. Mirgolbabaee, S. T. Ledari, N. M. Zadeh, and D. D. Ganji, "Investigation of the nonlinear equation of the circular sector oscillator by Akbari-Ganji's method," *Journal of Taibah University for Science*, vol. 11, no. 6, pp. 1110–1121, 2018.

[35] M. Sheikholeslami, M. Nimafar, and D. D. Ganji, "Nanofluid heat transfer between two pipes considering Brownian motion using AGM," *Alexandria Engineering Journal*, vol. 56, no. 2, pp. 277–283, 2017.

[36] D. D. Ganji, M. M. Peiravi, and M. Abbasi, "Evaluation of the heat transfer rate increases in retention pools nuclear waste," *International Journal of Nano Dimension*, vol. 6, no. 4, pp. 385–398, 2015.

[37] L. Kong, *Engineering Fluid Mechanics*, China Electric Power Press, Beijing, 1992.

[38] Q. M. Tan, *Dimensional analysis*, University of Science and Technology of China Press, Hefei, 2005.

[39] X. B. Zhang, *The research on performance of dynamic pressure type gas-oil separator in aero-engine*, Harbin Engineering University, Harbin, 2018.

[40] F. G. Blanchet, P. Legendre, and D. Borcard, "Forward selection of explanatory variables," *Ecology*, vol. 89, no. 9, pp. 2623–2632, 2008.

[41] J. J. Derksen, S. Sundaresan, and H. E. A. V. Den Akker, "Simulation of mass-loading effects in gas-solid cyclone separators," *Powder Technology*, vol. 163, no. 1-2, pp. 59–68, 2006.

[42] T. Hastie, R. Tibshirani, and R. J. Tibshirani, *Extended comparisons of best subset selection, forward stepwise selection, and the lasso*, 2017, http://arxiv.org/abs/170708692.

[43] N. M. Razali and A. H. Hashim, "Backward reduction application for minimizing wind power scenarios in stochastic programming," in *Power Engineering and Optimization Conference*, pp. 430–434, 2010.

[44] H. F. Shen, *Probability and statistics curriculum (fourth edition)*, Higher Education Press, Beijing, 2003.